

УДК 533.69.04

DOI: 10.26467/2079-0619-2018-21-1-124-136

IMPROVING THE AERODYNAMICS OF A TRANSPORT AIRCRAFT WING USING A DELTA PLANFORM WINGTIP LEADING EDGE EXTENSION

D. GUERAICHE¹, S.A. POPOV¹

¹*Moscow Aviation Institute (National Research University), Moscow, Russia*

The article explores the possibility of improving the aerodynamic properties of a supercritical-airfoil wing, typical for a modern passenger aircraft, using delta planform passive devices of large relative areas, installed along the leading edge at the wing tip. Delta extensions of various configurations were considered to be used as wingtip devices, potentially improving or completely replacing classical R. Whitcomb winglets. As a result of two- and three-dimensional CFD simulations performed on DLR-F4 wing-body prototype, the potential advantage of these devices was confirmed, particularly when they are installed in a combination with an elliptical planform, largely swept, raked winglet in terms of reducing the induced drag and increasing the aerodynamic lift-to-drag ratio at flight angles of attack. The growth in lift-to-drag ratio applying these devices owes it solely to the drop in drag, without increasing the lift force acting on the wing. In comparison to the classical winglets that lead to a general increase in lifting and lateral forces acting on the wing structure, resulting in a weight penalty, the Wingtip Ledge Edge Triangular Extension (WLETE) yields the same L/D ratio increase, but with a much smaller increase in the wing loading. A study has been made of the characteristics of the local (modified) airfoil in the WLETE zone in a two-dimensional flow context, and a quantitative analysis has been conducted of the influence of WLETE on both the profile and induced drag components, as well as its influence on the overall lift coefficient of the wing. The resulted synthesis of the WLETE influence on the wing L/D ratio will consist of its influence on each of these components. A comparison of the efficiency of using delta extensions against classical winglets was carried out in a multidisciplinary way, where in addition to the changes in aerodynamic coefficients of lift and drag, the increments of magnitude and distribution of the loads acting on the wing console were studied along with the maximum resulted structural stress. The study of the growth of structural stress on the wing structure after installing WLETE, confirmed the results obtained from CFD simulations that these delta extensions do not increase and do not change the distribution of total forces and moments acting on the wing console.

Key words: triangular extension, delta extension, wing leading edge, wingtip device, classical R. Whitcomb winglets, induced drag, supercritical airfoil, sharp wing leading edge.

INTRODUCTION

The year 2017 has seen the introduction of new models of single-aisle transport airliners – the Russian MS-21, Chinese Comac C919 and the Canadian Bombardier C S300, as well as refined versions of the well-established within the medium range segment of commercial aviation market liners – The Boeing B737 Max and Airbus A320 Neo. The ever fiercer competition for commercial aviation market share in this segment poses an increasingly urgent task for aircraft designers to optimize the future airliner aerodynamics with radically new approaches to improve fuel efficiency. In this regard, leading airframe manufacturers are conducting aggressive R&D aimed at further reducing the aerodynamic drag with minimal structural weight penalties. These R&D works are also driven by the emergence of revolutionary new CAE simulation software that allow for a comprehensive multidisciplinary optimization providing cost-effective solutions to problems adjacent to two or more physical phenomena, including traditional aircraft design tasks such as the interaction of gas dynamics with the wing cantilever, where, taking into account both manufacturing and operational limitations posed on the maximum allowable wingspan, the use of *complementary devices* has become mainstream such as wingtip devices, high-lift devices, root extensions and fairings of various shapes and sizes. In this research, we investigate a completely new wingtip device type for subsonic transport airplanes, in the form of a delta extension of the wing leading edge, installed right before the tip rib. In the course of computational experiments of air flow field near the wing and its loading, the relative advantage of these extensions against classical winglets has been revealed in terms of Lift-to-Drag ratio growth,

with a much smaller growth in the wing root bending moment and, as a result, lower total stress along the wing span and a much smaller structural weight penalty.

The idea of a 'polygonal' wing leading edge with a forward triangular-like protrusion existed long time before the first powered flight of a heavier-than-air aircraft, although it was basically a reflection of several attempts to imitate bird wing shapes without neither theoretical nor experimental understanding of its effects due to the immature aerodynamic science of the XIX century. Very soon after powered flight of a heavier-than-air aircraft became a reality, the structural layout of airplanes has become increasingly complex to meet few practical design requirements and their velocities grew exponentially. Combined with the technical non-practicality and non-feasibility of the flapping wing, this has led to the phenomena of bird flight to remain not fully studied till our days. However, few elements of bird wings periodically offer inspiration for aircraft designers looking for novel solutions to traditional problems such as the induced drag of a transport airliner, responsible for as much as 40% of the total aerodynamic drag. Few examples of bio-inspired solutions to this problem include multiple-elements winglet design [1], M- or W-wing planform transonic aircraft studied at NASA [2], the European project SARITSU ("Smart" aircraft structures) in which TsAGI institution is currently involved. Despite the fact that since the beginning of the second half of the XX century, a layout with the minimum induced drag was identified: the so-called Prandtl Plane, featuring a lifting fuselage with a closed wing [3]. Just like the flapping wing, this layout was found to be (and is still today) technically non-feasible. As a result, since the mid-1970s, alternative solutions to "heal" the wingtip local flow field are being developed, including geometric and aerodynamic twist, various configurations wingtip devices and the concept of adaptive wing. As long as these alternatives offer only insignificant Lift-to-Drag ratio increase of no more than 5-7 % at flight angles of attack, the problem of induced drag reduction persists to be a central objective in the aerodynamic shape optimization of commercial airliners. In the Department of Aerodynamics at Moscow Aviation Institute, a new potentially efficient solution to this problem has been both CFD and experimentally investigated. This solution, consisting of a wingtip device in the form of a triangular extension retrofitted to a low-speed seaplane demonstrator with floats [4-7], revealed a small improvement in the wing Lift-to-Drag ratio at flight angles of attack. The logical continuation of this research would be testing this same concept at much higher velocities (few geometry corrections are required to adapt the extensions to the high velocity flow field), which has been performed in this article. The results of CFD experiments are presented, that were performed on high subsonic transport aircraft prototype DLR-F4, equipped with wingtip leading edge triangular extension (WLETE). As a result, an increased local pressure on the upper surface of the wing near WLETE was observed (Fig. 10b), which equilibrates low pressure on top surface near the wing tip with the high pressure on the lower wing surface and weakens the pressure difference at the wing tip, thus reducing the wingtip vortex intensity. This in turn leads to a significant reduction the induced drag of the wing, but the increase in L/D ratio, as during the wind tunnel tests of the WLETE-equipped seaplane [4], turned out to be insignificant (Fig. 12), evidently due to the drop of lifting properties in the wing sections along WLETE, where the top and bottom pressures has been equilibrated. In order to compensate the losses of C_l along WLETE sections, a decision was made to equip the tip of the wing, immediately after WLETE, with a lifting horizontal (raked) winglet featuring the same airfoil as the wing tip section. This lifting raked winglet features an increased sweep angle to balance the forward-shift of the aerodynamic center due to the leading edge extension and its pitching moment (this becomes particularly important at large angles of attack). Besides, this raked winglet has an elliptical planform to minimize its own induced drag (its side effect), see Fig. 11. This combination of WLETE with a raked elliptical winglet resulted in L/D increase at flight angles of attack, comparable to the increase produced by classical Whitcomb winglets, but with much less additional loads on the wing structure (Fig. 13). This can be explained by the almost unchanged values of total lifting and lateral forces acting on the wing: the span of the additional lifting raked winglet was tuned so that its (additional) lift force was close to the total loss of lift due to WLETE. Thus, in comparison with Whitcomb winglets (where the L/D ratio grows simultaneously due to the growth of C_l and the drop in the induced component of C_d), here we have a drop in drag without a lift 'penalty' (and as a consequence – without a wing root bending moment penalty). Similar technical solutions of a wingtip device in the form of a com-

bination of a triangular extension and an extensively swept winglet have been recently tested on the blades of experimental helicopters: The Russian project PSV (Perspective High Speed Helicopter) and the European Blue Copter project [8], see Fig. 1a and b below. Optimization of blades' plan form in recent jet engines' fan blades also led to a similar concept, for example, on Rolls-Royce LEAP engine fan blade (Fig. 1c).

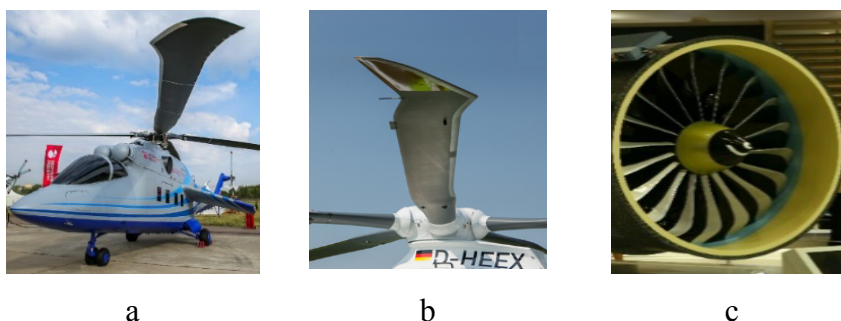


Fig. 1. The use of a leading edge triangular extension as a wingtip device in combination with a raked winglet on helicopter blades:
a – Russian PSV project, b – European Blue Copter,
c – A similar concept can be seen on Rolls-Royce LEAP fan blade

ANALYSIS OF CURRENT STATUS OF THE ISSUE

- *Three-dimensional flow field around a typical transport aircraft wing:*

In order to get a deep insight into the flow field near the wing, a computational simulation of DLR-F6 passenger aircraft wing-body prototype was performed using ANSYS Fluent CFD software. In Fig. 2, shown is the typical picture of the flow field around a passenger airplane at a moderately high angle of attack, where we can notice an interference with the fuselage body, with the engine pylon and nacelle, and a general transverse flow from the wing root to its tip along the entire wing span, which then gets accumulated into a vortex sheet downstream the wing tip, with a larger intensity, the higher is the angle of attack α . The flow field can be generally divided into four characteristic zones (Fig. 2):

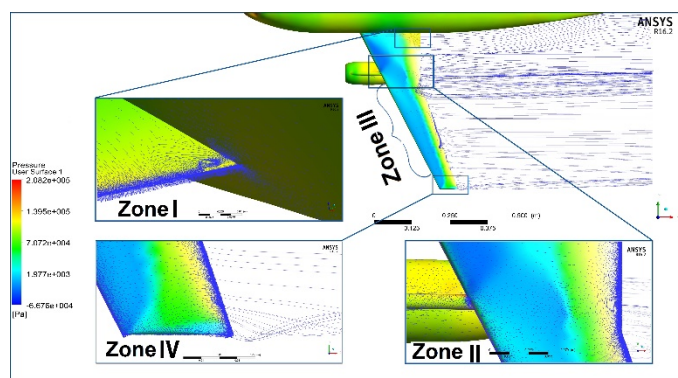


Fig. 2. CFD flow field visualization near the wing of passenger aircraft prototype DLR-F6, allowing the identification of typical characteristic zones within the flow field

Zone I of fuselage influence: immediately in the wing junction area to the fuselage, due to the trailing air behind the wing adhering to the fuselage surface, a pressure difference occurs at the junction of the trailing edge of the wing, which leads to an upstream flow and the formation of a minor vortex. To reduce interference drag in this zone, it is usually enough to install large span wing root fairings, together with the belly fairing.

Zone II of engine influence: manifests itself mainly at angles of attack larger than $\alpha \geq 3^\circ$, due to the shading effect of the wing root section by the engine nacelle. In addition, the presence in this Zone

II of the abrupt change of the wing trailing edge sweep angle, that causes a noticeable upstream flow along the upper surface of the wing. Here we can suggest a smoother transition, for example, in the form of a large radius fillet.

Zone III: the flow here can be approximately assumed to be two-dimensional, in view of the absence of interferences and weak transverse flow, a quasi-constant local angle of attack spanwise. This zone is responsible for a significant portion of lift force of the wing, and it is wider the larger is the wing aspect ratio.

Zone IV of wingtip vortex influence: Here the flow is deeply three-dimensional, where already from the middle of the tip chord, the overflow of high-pressure air from the lower surface of the wing into the upper takes place and, as a result, its pressure increases to some extent, and equilibrates downstream with the high pressure of the lower surface near the trailing edge, where the tip vortex takes shape with a low pressure core of the vortex (see Fig. 10a), which in turn draws even more transverse flow from the tip sections of the wing. This effect causes a loss of efficiency of the tip sections, and is chiefly responsible of the induced drag of a finite span wing. The zone IV extends spanwise to cover a larger area, the larger the angle of attack is. At angles of attack exceeding the critical $\alpha_{cr.}$, this zone can cover up to a half of the wingspan (Fig. 3b). Commonly used methods for controlling the formation of Zone IV at moderate α and its rapid growth at larger α include increased wing aspect ratio, twist and various wingtip devices. Recently, a new method is being investigated – the use of a half-W-wing planform, where a decreased angle of sweep of the $\frac{1}{4}$ tip part of the wing with the purpose of preliminarily diverting the transverse flow from flowing from root to the tip. On 26.09.2017, an A330 flying testbed with a modified tip section of $\frac{1}{4}$ wing span took off within the framework of the European project BLADE (Breakthrough Laminar Aircraft Demonstrator in Europe, Fig. 3a). In addition to the reduced sweep, the A330 BLADE wing end sections feature a laminar airfoil. The concept of the leading edge extension WLETE studied in this paper, may also be viewed from the point of view of local sweep of the end sections along the extension and from the point of view of two-dimensional flow around the modified (with an elongated and sharpened leading edge) airfoil in WLETE sections (see the two-dimensional formulation of the problem below).

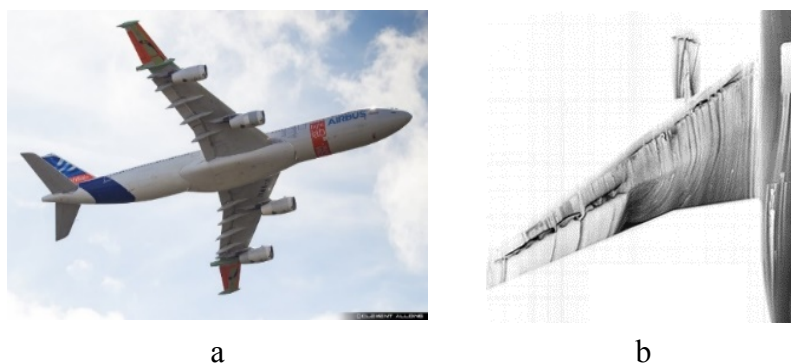


Fig. 3. a – A330 flying test bed within the European project BLADE featuring a lowered sweep tip section with a laminar airfoil;
b – Surface flow visualization at an angle of attack near the critical $\alpha \sim \alpha_{cr.}$, showing flow separation taking place at the tip Zone IV, which then covers nearly half of the wing span

WINGTIP LEADING EDGE TRIANGULAR EXTENSION AS A WINGTIP DEVICE

- Description of DLR-F4 wing-body model and the geometry of the investigated tip extension:

The use of a triangular extension as a wingtip device is obviously aimed at improving the local flow field near the wingtip Zone IV. In order to isolate the influence of the engine nacelle and its mounting pylon at Zone II, and to study the influence of the delta extension on the aerodynamics of the "clean" wing, DLR-F4 wing-body prototype was selected as an experimental platform (Fig. 4).

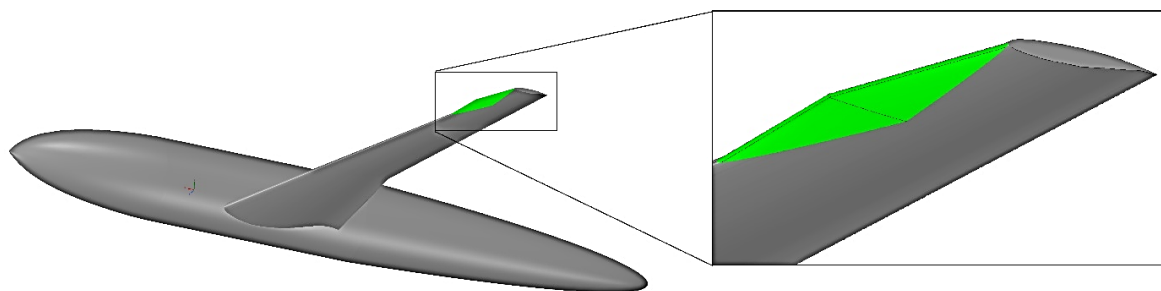


Fig. 4. CAD model of DLR-F4 passenger aircraft wing-body prototype, shown equipped with a leading edge delta extension in the wingtip

Unlike the extension installed on the wing of the seaplane wind tunnel model described in [4], featuring a virtually constant shape of the leading edge along the entire span of the extension, which is close to the shape of the main wing leading edge, the delta extension studied here is conical: featuring an almost point-sharp nose leading edge with an extremely small radius in the center plane of the extension, and gradually increasing the leading edge radius, the closer to the end of the delta extension, so that at the right and left end points of the extension, the leading edge radius is equal to the main wing leading edge radius (Fig. 5, section C-C). The extension is built by "pulling forward" the leading edge of the wing to a distance of about $\frac{1}{5}$ -th of the chord length in the center plane of the extension (the central plane of the extension is parallel to the plane XY of the aircraft, but is not the extension's symmetry plane, due to the sweep of the wing) (Fig. 5, plan view). The central plane in section A-A is located approximately at a distance from the tip chord of about $\frac{1}{10}$ -th of the half-span of DLR-F4 wing. The delta extension span in the first approximation was selected to be $\frac{1}{5}$ -th of the leading edge length of one DLR-F4 wing console. In every cross-section along the extension, its upper and lower surfaces are tangent to respectively the upper and lower surfaces of the main wing surface. The leading edges of the extension are straight lines spanwise.

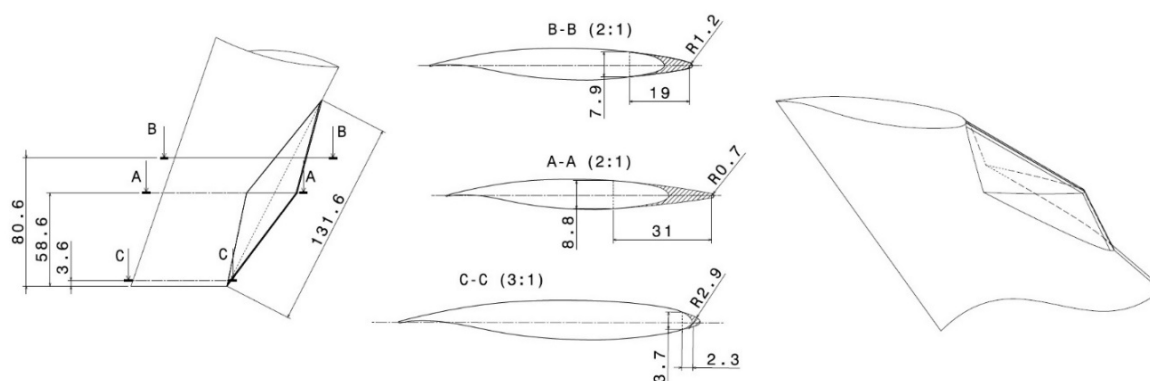


Fig. 5. Plan view, isometric view and sections along the investigated delta extension device, installed along the leading edge of a DLR-F4 wing tip (dimensions shown in millimeters)

From the delta extension's central section A-A in Fig. 5, it is clear that the addition of the delta extension leads to a retreat from the supercritical airfoil shape, optimal for high subsonic and transonic velocities to a "faster" airfoil with a sharpened, almost "supersonic" leading edge in this section A-A, and smoothly shifting back to the initial airfoil shape the further from the central section we move. The new airfoil, although less optimal for a subsonic passenger airplane wing, its [local] use at the tip sections allows us to decrease the loading on Zone IV and decrease the pressure difference near the wing tip. Also, its [profile] drag is noticeably smaller than that of the initial airfoil (see Fig. 6b below). Thus, in the Zone IV, when the triangular extension is installed, we get a drop in both the lifting force (Fig. 6a) and the drag force.

- *Two-dimensional formulation of the problem of comparing the characteristics of the modified airfoil along the extension sections with the initial one:*

In Fig. 6 below shown is a comparison of the coefficients of lift and drag forces of the original airfoil (DFVLR-R4) with the new airfoil in the central section A-A at different angles of attack. Over the whole range of angles of attack, with the exception of large negative, noticeable is the overall fall in both C_d and C_l to a greater extent, the greater is the angle of attack.

From Fig. 6c, we can conclude that with increasing α , C_d falls faster than C_l , and as a result, at positive α , the Lift-to-Drag ratio $L/D = C_l / C_d$ of the modified airfoil turns out to be higher than that of the initial one.

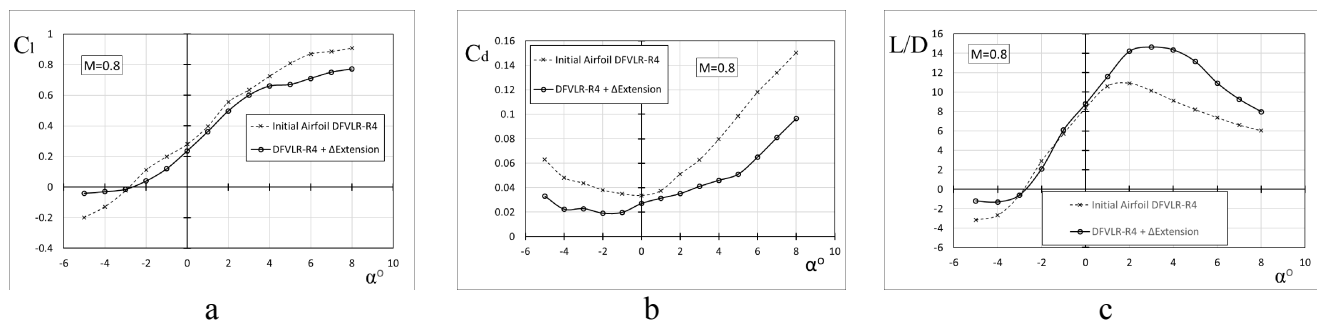


Fig. 6. Dependences of the coefficients of lift (a), drag (b) on the angle of attack α for the initial airfoil DFVLR-R4 and for the modified airfoil at A-A section along the delta extension. c – Dependence of L/D ratio on the angle of attack

In order to explain the given in Fig. 6 above dependencies, the pressure field near the airfoils was studied at a small (Fig. 7) and at a large (Fig. 8) angles of attack α .

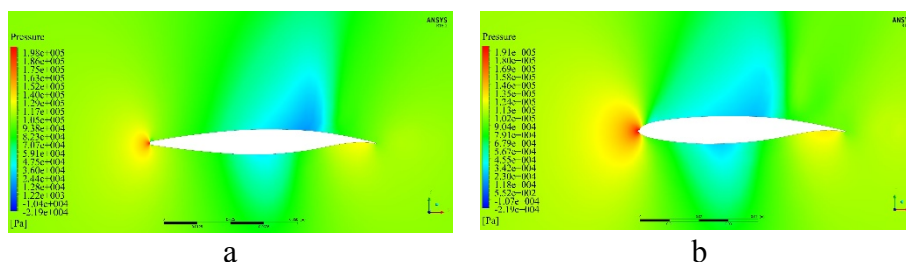


Fig. 7. Pressure field at section A-A along the delta extension central plane – a comparison between the modified airfoil (a) and the initial DFVLR-R4 (b) at $M = 0.8$ and a small angle of attack of $\alpha = 1^\circ$

From Fig. 7 above, the installation of the delta extension leads to the fact that, at small α , the high-pressure stagnation area immediately ahead of the stagnation point has become much smaller, which reduces the pressure component of the drag $C_{d_{pr}}$, and partially explains the general fall of C_d . However, the zone above the extension, and downstream up until the middle of the chord length, is less discharged than in the analogous zone of the original airfoil, which explains the loss in the values of lift coefficient C_{ya} . With increasing α , the extension becomes lifting due to the emergence of a small discharged zone above its leading edge (see Fig. 8a below), and a slight shifting of the high-pressure stagnation zone moving towards the zone below the extension. This effect somewhat slows down the fall of C_l , but despite this, the losses in C_l values are the more significant, the higher the angle of attack (Fig. 6a) because of the significant narrowing of the discharged zone on the upper surface of the airfoil, from which the delta extension "cuts" almost the entire front half of the chord length. Becoming lifting, the leading edge of the delta extension, in combination with the less lifting (as compared to the initial airfoil) middle and back of the chord length, creates a noticeable forward-shift of the aerodynamic center, and an increasingly large pitching moment with increasing the angle of attack.

It should be noted that the emergence of a lifting force on the delta extension at moderately large α is due to the rounded leading edge which, despite the very small radius of curvature in the central section A-A, allows the flow to stay attached to the upper surface of the airfoil without separation. This en-

asures a continuous attached flow downstream (the velocity vectors near the nose of the extension are shown zoomed up in Fig. 8a). CFD test of a delta extension with a sharp wedge-shaped leading edge (along the entire span of the extension) showed slightly better gains in drag C_d , but losses in lift C_l however, turned out to be an order of magnitude larger due to the "non-lifting" delta extension and a full flow separation at large α (see [9, 10] for details on the effect of a sharp leading edge in a subsonic flow field).

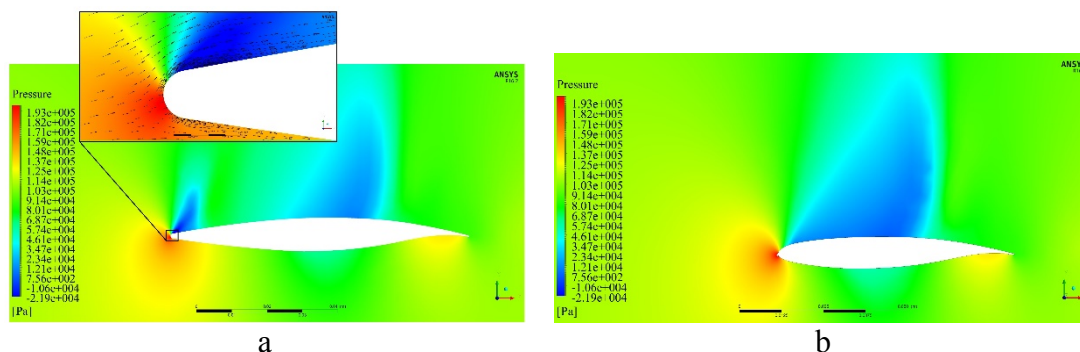


Fig. 8. Pressure field in section A-A along the extension's central plane – a comparison between the modified airfoil (a) and the initial airfoil DFVLR-R4 (b) at a high angle of attack $\alpha = 4^\circ$, $M = 0.8$

- Three-dimensional CFD simulation results of DLR-F4 model equipped with triangular extension:

As during the analysis of the two-dimensional flow, visualization of the three-dimensional pressure field on the upper surface of the wing shows an increase in pressure near the delta extension at small α (Fig. 9a and b), and its equilibration with the high pressure on the lower surface. Local high pressure above the extension serves as an obstruction to the transversal flow, preventing it from further flowing towards the tip, thereby the pressure difference is reduced in its vicinity. This reduces the intensity of the wingtip vortex, which can be estimated through the streamlines and the velocity vectors' length (depicting local velocity values) in the plane behind the wing. The color of the velocity vectors behind the wing (local pressure) indicates a drop in the pressure gradient from the vortex core to its periphery. This simultaneously leads to a noticeable reduction in induced drag, and to a fall in the lift C_l of tip sections along the extension. As a result, the L/D ratio only insignificantly grows at small angles of attack $\sim 3\%$ (see the graph in Fig. 11c). At a moderately large angle of attack $\alpha \sim 4^\circ$ (Fig. 9c and d), we can notice the emergence of a discharged zone on the upper surface of the delta extension, which now becomes lifting, thus softening the losses in lift coefficient C_l at moderately high α (graph at Fig. 11a). However, this does not greatly improve the L/D ratio gain from the extension, up to $\sim 5\%$ (the graph in Fig. 11c).

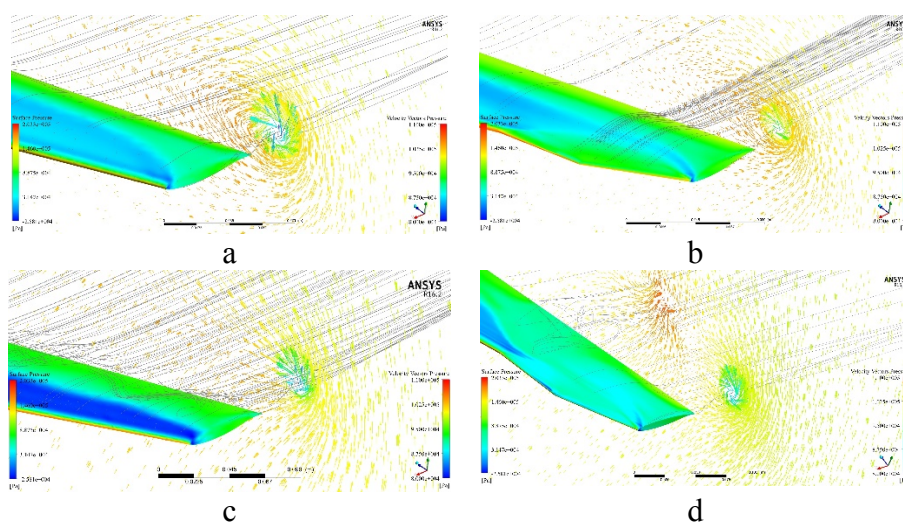


Fig. 9. The pressure field on the wing top surface at $M = 0.8$: a – Initial DLR-F4 wing at $\alpha = 1^\circ$, b – DLR-F4 wing equipped with a delta extension at $\alpha = 1^\circ$, c – Initial DLR-F4 wing at $\alpha = 4^\circ$, d – DLR-F4 wing with extension at a high $\alpha = 4^\circ$

- Compensation of the loss in the wing lifting properties caused by the delta extension, using a complementary lifting raked winglet:

Based on the two-dimensional formulation of the problem and the picture of three-dimensional flow, we can conclude that the installation of a leading edge delta extension allows an increase in the aerodynamic Lift-to-Drag ratio of DLR-F4 model at a certain value:

$$\Delta(L/D)_{\Delta Ext.} = (L/D)_{DLR-F4+\Delta Ext.} - (L/D)_{DLR-F4_Initial} \quad (1)$$

A part of this increase is due to the fall of C_d : $\Delta(L/D)_{\downarrow C_d}$, where a part of the fall of C_d that results from the fall of its induced fraction is in turn due to the losses in C_l , which on the contrary lead to a drop in overall L/D ratio by a certain value $\Delta(L/D)_{\downarrow C_l}$. Then, after installing the delta extension, the L/D ratio of the model experiences an increment by an amount:

$$\Delta(L/D)_{\Delta Ext.} = \Delta(L/D)_{\downarrow C_d} - \Delta(L/D)_{\downarrow C_l} \quad (2)$$

On the other hand, the L/D ratio of the model equipped with the delta extension is equal to:

$$(L/D)_{\Delta Ext.} = \frac{C_{l_initial} + \Delta C_{l_{\Delta Ext.}}}{C_{d_initial} + \Delta C_{d_{\Delta Ext.}}} \quad (3)$$

where $\Delta C_{l_{\Delta Ext.}}$ and $\Delta C_{d_{\Delta Ext.}}$ are the increments (decrease) in the values of respectively C_l and C_d of the model, due to the presence of the delta extension. In (3) it is possible to expand the profile and induced components of the increment of the drag coefficient: $\Delta C_{d_{\Delta Ext.}} = \Delta C_{d_{\Delta Ext. _ prof.}} + \Delta C_{d_{\Delta Ext. _ ind.}}$. The induced drag in turn can be expressed through the lift C_l and the wing aspect ratio λ through the well-known dependence: $C_{d_ind.} = \frac{C_l^2}{\pi \cdot \lambda \cdot e}$. Neglecting minor increments in the wing aspect ratio λ , and its geometric coefficient e after installing the delta extension, the denominator is constant, let's denote it: $\pi \cdot \lambda \cdot e = \text{const} = P$, then the drop of the induced component of $\Delta C_{d_{\Delta Ext.}}$ is linked to the drop in the lift coefficient as follows: $\Delta C_{d_{\Delta Ext. _ ind.}} = \Delta C_{l_{\Delta Ext.}}^2 / P$, substituting in (3):

$$(L/D)_{\Delta Ext.} = \frac{C_{l_initial} + \Delta C_{l_{\Delta Ext.}}}{C_{d_initial} + \Delta C_{d_{\Delta Ext. _ prof.}} + [\Delta C_{l_{\Delta Ext.}}^2 / P]} \quad (4)$$

Equation (4) represents a quantitative juxtaposition of gains from the delta extension, manifested in the drop of profile drag $C_{d_{\Delta Ext. _ prof.}}$ ($\Delta C_{d_{\Delta Ext. _ prof.}}$ – always negative, see Fig. 6b) and the losses of this wingtip device from the fall in lift C_l ($\Delta C_{l_{\Delta Ext.}}$ – is negative at all flight α , see Fig. 6a). In (4) we can notice the presence of the square of $\Delta C_{l_{\Delta Ext.}}$ in the denominator, which leads to a rapid fall of $(L/D)_{\Delta Ext.}$ ratio, together with the [negative] $\Delta C_{l_{\Delta Ext.}}$ in the numerator. In other words, reducing the lift force, although yields induced drag reductions, has a double negative effect on L/D ratio and therefore, even small losses of the lift coefficient are able to completely cancel any gains obtained from profile drag reductions. This is what happened during CFD simulations of a ‘non-lifting’ wedge shaped

supersonic-leading-edge delta extension. Thus, the highest L/D ratio of the delta-extension-equipped model $(L/D)_{\Delta Ext.} \approx \max$ corresponds to the minimum drop of lift $\Delta C_{l_{\Delta Ext.}} \approx \min$. This means that, given a possibility to somehow fully compensate the C_l loss, reducing to zero $\Delta C_{l_{\Delta Ext.}} = 0$, from (4) we can obtain the maximum possible L/D ratio of the delta-extension-equipped model, caused exclusively by the drop of the profile component of the drag coefficient:

$$(L/D)_{\Delta Ext.}^{\max} = \frac{C_{l_initial.}}{C_{d_initial.} - |\Delta C_{d_{\Delta Ext. _prof.}}|} \quad (5)$$

In this case, the maximum possible L/D ratio growth can be obtained from (2): $\Delta(L/D)_{\Delta Ext.}^{\max} = \Delta(L/D)_{\downarrow C_d} - \Delta(L/D)_{\downarrow C_l}^0 = \Delta(L/D)_{\downarrow C_d_prof.}$

An obvious solution to compensate the fall of lift C_l would be increasing the wing plan area. However, a simple ‘wing extension’ naturally leads not only to an additional lift force, but also to an additional profile and induced drag (the price for any additional lift). Thus, it is necessary to finely tune the geometry of the additional part for it to have a minimum possible *own induced drag*. It is well known that the minimum induced drag planform is elliptical. Also, in order to simultaneously minimize its *own profile drag* and balance the forward-shift of the aerodynamic center and the pitching moment caused by the extension, the lift-compensating part should be performed with the maximum possible sweep.

In Fig. 10 below, shown is the pressure field and streamlines over the wing of a DLR-F4 equipped with the delta extension and an additional lifting (horizontal) raked winglet of an elliptical planform, featuring the same airfoil as the wing end chord at its root, and smoothly reducing to a point-small tip chord with the purpose of maximum narrowing of the contact zone between lower and upper air flows with different pressures, which also minimizes the induced drag. This raked winglet features an increased sweep as compared with the main wing. In comparison with the flow patterns shown earlier at Fig. 9 of the clean wing, as well as the wing with a delta extension, we can notice a significant drop in the vorticity in the plane behind the wing, and a smoother pressure distribution including at large angles of attack (Fig. 10b).

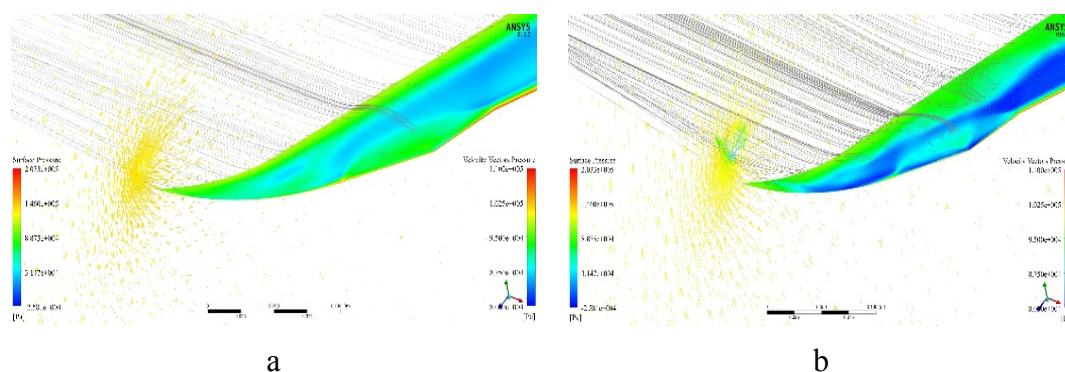


Fig. 10. Top surface pressure field on DLR-F4 wing equipped with a delta extension and a lift-compensation raked winglet at $M = 0.8$ and angles of attack: a – Small $\alpha = 1^\circ$, b – High $\alpha = 4^\circ$

From the shown in Fig. 11 below dependences on the angle of attack of aerodynamic coefficients, we can notice the favorable effect of the delta extension on DLR-F4 wing aerodynamics, which is manifested in a much greater extent, after retrofitting it with a lift-compensation raked winglet, which restores (with acceptable losses in C_d) the initial values of C_l (Fig. 11a and b), and thus allowing to get an overall gain in L/D ratio of 6 to 13%, which is close to, or even exceeds the gains obtained using traditional Richard Whitcomb winglets [11–13].

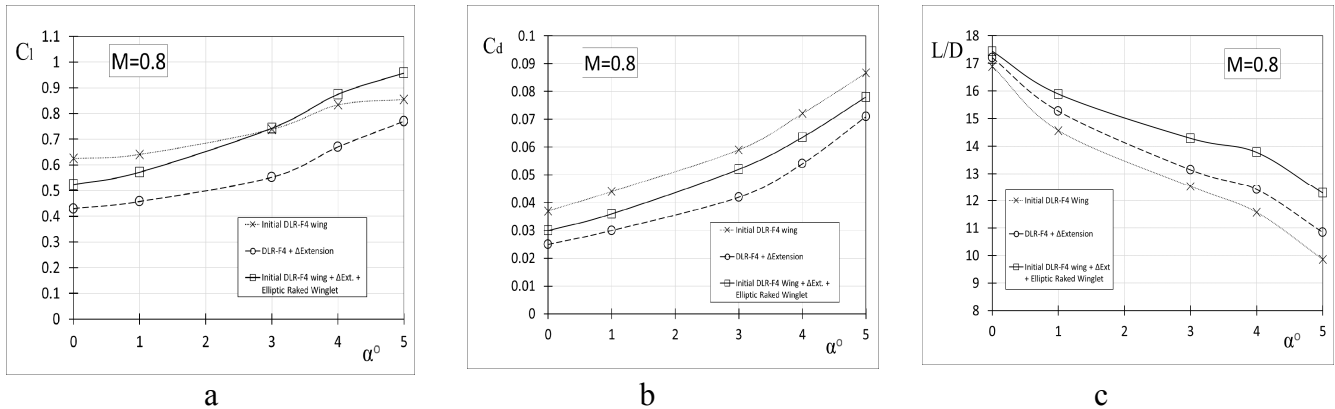


Fig. 11. Dependences of coefficients of the lift force (a), the drag force (b) and the L/D ratio (c) on the angle of attack α for the initial DLR-R4 wing, the wing equipped with a delta extension and for the final model with the delta extension and the lift-compensation, elliptic planform raked winglet

- Efficiency of the delta extension as a wingtip device in comparison with classical winglets:

In Fig. 12 below, shown are the values of maximum total Von Mises stress, and its spanwise distribution for the initial DLR-F4, as well as for DLR-F4 equipped with different wingtip devices. Confirming the CFD simulation conclusions, that the addition of the delta extension in combination with the lift-compensation raked winglet does not increase, and does not change the distribution of forces and moments acting on the wing console, in Fig. 12d, it can be seen that this new wingtip device virtually does not change the total wing loading and structural stress (the growth of stress is only 1.83% versus 24% growth from classical winglets). Thus, this newly developed delta extension wingtip device can be retrofitted to the wings of operational airplanes without the need for a structural rework of the wing console.

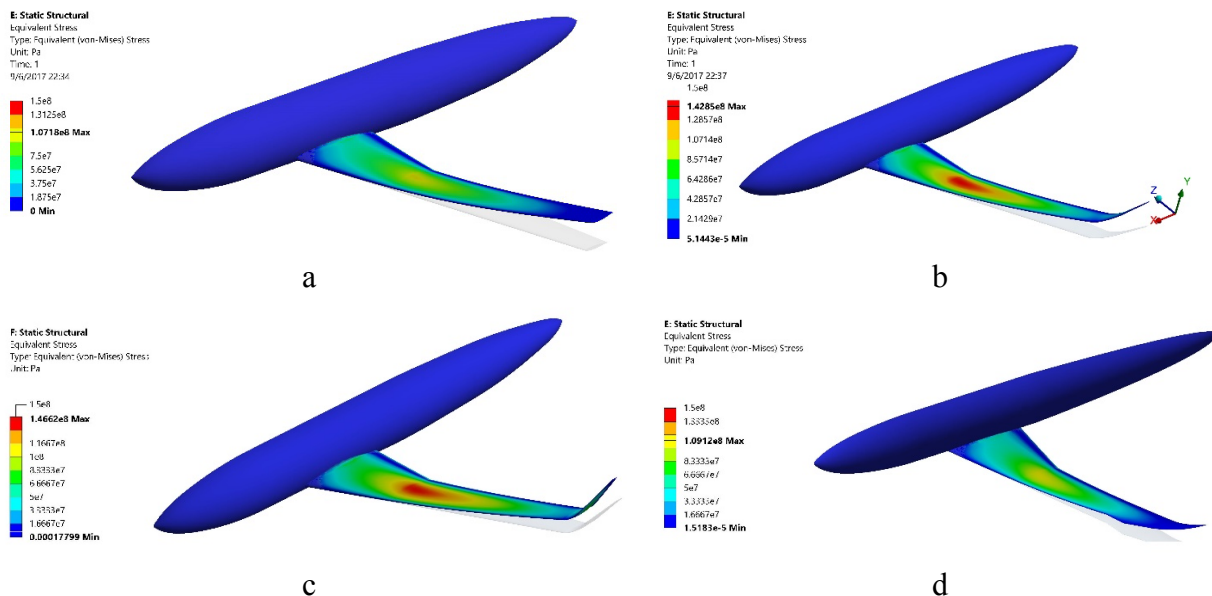


Fig. 12. Spanwise distribution and magnitude of maximum Von-Mises stress of the wing console at $M = 0.8$ and $\alpha = 1^\circ$:
a – Initial DLR-F4 model; b – DLR-F4 + classical winglet with a large cant angle of $\psi = 75^\circ$;
c – DLR-F4 + winglet with a moderate cant angle of $\psi = 45^\circ$; d – DLR-F4 + delta extension + lifting elliptic raked winglet

CONCLUSION

This article provides an original multidisciplinary investigation of an innovative method of reducing the induced and profile components of the drag of a high-subsonic passenger aircraft wing with

a supercritical airfoil, without increasing and without significant redistribution of the wing loading. This technical solution is quite simple to implement airplanes in operation, and consists in ‘covering’ the wing leading edge right close to the wing tip, with a triangular planform extension, without modifying the local geometry of the wing or the wing box structure. These devices allow drag reductions due to a double effect: on one hand, the ‘two-dimensional’ profile drag is reduced due to the transition to a new airfoil shape with an elongated and sharpened leading edge. On the other hand, the locally modified airfoil, having a lower lift coefficient compared to the initial supercritical airfoil, allows simultaneously to reduce the induced, ‘three-dimensional’ drag by reducing loading on the wing tip sections. Induced drag is reduced through balancing the pressure difference of the upper and lower surfaces of the wing before the transverse flow coming from the root of the wing reaches the tip sections. As a result, the pressure difference near the tip becomes smaller, which significantly reduces the intensity of the wingtip vortex and the induced drag. All these advantages of wingtip triangular extensions were revealed during low-speed wind tunnel tests of the seaplane demonstrator last year at T-1 wind tunnel of Moscow Aviation Institute.

The novelty of this work lies in the multifold revision of the concept of the leading edge delta extension proposed earlier and its adaptation to a transonic flow mode in order to obtain from it not only a drop in drag, but also an increase in overall aerodynamic Lift-to-Drag ratio (which is, matter of fact, the final goal of using this concept). The solution, which consists in retrofitting the refined delta extension with a lifting raked winglet, was found after a profound analysis of the change in both the two-dimensional and three-dimensional flow patterns near the extension. Visualizations of the change in the local pressure field on the upper and lower surfaces of the wing made it possible to estimate the losses of lift in the delta extension sections, and calculate the necessary size of the lift-compensation raked winglet. This raked winglet, not only restores the previous level of the wing lift coefficient, but is also used to balance the forward shift of the aerodynamic center and the pitching moment generated by the extension. To do this, it is sufficient to increase its sweep angle. In order to minimize its side effect inherent in its own induced drag, we decided to give it an elliptic planform and a point-small chord length at its tip.

The resulting combination of a triangular extension with an extensively swept back, elliptic planform lifting raked winglet allowed us to obtain approximately the same Lift-to-Drag ratio increase at typical flight flow conditions, as when installing a classical Whitcomb winglet, but without increasing the load on the wing structure, keeping unchanged the total lift and lateral forces acting on the wing console. This advantage is very important for the implementation of this concept on operational airplanes, since it requires almost no efforts to upgrade the design or strengthen the wing structure.

REFERENCES

1. **La Roche U., La Roche H.L.** Induced Drag Reduction using Multiple Winglets, looking beyond the Prandtl-Munk Linear Model. 2nd AIAA Flow Control Conference, 2004. DOI: 10.2514/6.2004-2120
2. **Edward J.B. W.** Free Flight Measurements of the Drag and Longitudinal Stability of a Transonic M-Wing Aircraft. Bedford Library, 1964.
3. **D.A.J. van Ginneken, Mark Voskuil, Michel J.L. van Tooren.** Automated Control Surface Design and Sizing for the Prandtl Plane. AIAA 2010. DOI: 10.2514/6.2010-3060
4. **Popov S.A., Gueraiche D., Kuznetsov A.V.** Experimental study of the aerodynamics of a wing with various configurations of wingtip triangular extension. Russian Ae ronautics (Iz VUZ). July 2016, Vol. 59, Issue 3, pp. 376–380. DOI: 10.3103/S1068799816030132
5. **Sakornsin R.** *Optimizatsiya aerodinamicheskogo oblika kryla gidrosamoleta s poplavkom na kontse* [Optimization of the Aerodynamic Shape of a Seaplane Wing with Floats on its Tips]. Trudy MAI, Issue 57, 2012.

6. **Sakornsin R.** *Uluchsheniye aerodinamicheskikh kharakteristik kombinirovannogo kryla putem dobavleniya treugol'nogo vystupa* [Improving the Aerodynamic Characteristics of a Combined Wing by Equipping it with a Triangular Extension]. Trudy MAI, Issue 65, 2013.

7. **Sakornsin R.** *Aerodinamicheskii kharakteristiki kryla s vystupom pri raznykh uglakh otkloneniya vystupov i razlichnykh komponovkakh kryla gidrosamoleta v mestakh soyedineniya* [The Aerodynamic Characteristics of the Wing with an Extension at Different Setting Angles of the Extension and Various Layouts of the Seaplane Wing Junction Area]. Trudy MAI, Issue 70, 2013.

8. **Johnson C.S., Barakos G.N.** Optimizing Rotor Blades with Approximate British Experimental Rotor Program Tips. Journal of Aircraft, Vol. 51, № 2, 2014. DOI: 10.2514/1.C032042

9. **Kandil O.A., Mook D.T., Nayfeh A.H.** Subsonic Loads on Wings having Sharp Leading Edges and Tips. Journal of Aircraft, 1976, Vol. 13, N 1. DOI: 10.2514/3.44512

10. **Fung Y.C.** On the Behavior of a Sharp Leading Edge. Journal of the Aeronautical Sciences, 1953, Vol. 20, pp. 644–645. DOI: 10.2514/8.2773

11. **Whitcomb Richard T.** A Design Approach and Selected Wind Tunnel Results at High Subsonic Speeds for Wing-tip Mounted Winglets. NASA Technical Note D-8260. 1976.

12. **Nicolas R. El Haddad and Luis Gonzalez.** Aerodynamic Design of a Winglet for the Dassault Falcon 10. AIAA 2016. DOI: 10.2514/6.2016-0776

13. **Takenaka K., Hatanaka K., Yamazaki W., Nakahashi K.** Multidisciplinary Design Exploration for a Winglet. AIAA Journal of Aircraft, 2008. DOI: 10.2514/1.33031

INFORMATION ABOUT AUTHORS

Djahid Gueraiche, Postgraduate and Research Assistant of Aircraft Aerodynamics and Heat Transfer Chair of Moscow Aviation Institute, guaero.tech@gmail.com or d.gueraiche@mai.ru.

Sergey A. Popov, Candidate of Sciences (Physics and Mathematics), Assistant Professor of the Aircraft Aerodynamics and Heat Transfer Chair of Moscow Aviation Institute, flowmech@gmail.com.

УЛУЧШЕНИЕ АЭРОДИНАМИКИ КРЫЛА ПАССАЖИРСКОГО САМОЛЕТА С ПОМОЩЬЮ ЗАКОНЦОВКИ ТРЕУГОЛЬНОЙ ФОРМЫ В ПЛАНЕ

Д. Гуереш¹, С.А. Попов¹

¹Московский Авиационный Институт (национальный исследовательский университет),
г. Москва, Россия

В статье изучена возможность улучшения аэродинамических характеристик типичного крыла пассажирского самолета со сверхкритическим профилем с помощью пассивных устройств треугольной формы в плане большой относительной площади, установленных на передней кромке в концевой части крыла. Рассмотрено использование треугольных выступов различных конфигураций в виде концевых устройств, потенциально усовершенствующих либо полностью заменяющих классические законцовки типа винглет Уиткомба. В результате плоского и трехмерного численного моделирования обтекания модели прототипа крыла-корпуса DLR-F4, было подтверждено потенциальное преимущество данных устройств, особенно в совокупности с эллиптической несущей законцовкой большой стреловидности, в плане снижения индуктивного сопротивления и роста аэродинамического качества на полетных углах атаки. Рост качества при применении данных устройств обусловлен исключительно падением сопротивления, без увеличения подъемной силы крыла. В сравнении с классическими законцовками, увеличивающими подъемную и боковую силу на конструкцию крыла, треугольный выступ дает такой же рост качества, но при гораздо меньшем росте нагрузок на конструкцию крыла. Приведено исследование характеристик местного, модифицированного, профиля в зоне выступа в двумерной постановке, и количественный анализ влияния выступа как на профильную и индуктивную составляющие сопротивления, так и на общую подъемную силу крыла. Синтез влияния выступа на аэродинамическое качество крыла сложится из его влияния на каждую из этих составляющих. Сравнение эффективности применения треугольного выступа с классическими законцовками было проведено в многодисциплинарной постановке задачи, где помимо коэффициентов подъемной силы и силы сопро-

тивления были получены изменения величины и распределения нагрузок, действующих на консоль крыла, и максимальных напряжений. Исследование роста нагрузок на конструкцию крыла после установки треугольного выступа подтвердили полученные из вычислительной гидродинамики выводы о том, что выступ не увеличивает и не меняет распределение суммарных сил и моментов, действующих на крыло.

Ключевые слова: треугольный выступ, передняя кромка крыла, концевое устройство, классическая законцовка, винглет Р. Уиткомба, индуктивное сопротивление, сверхкритический профиль, острая передняя кромка.

СПИСОК ЛИТЕРАТУРЫ

1. **La Roche U., La Roche H.L.** Induced Drag Reduction using Multiple Winglets, looking beyond the Prandtl-Munk Linear Model. 2nd AIAA Flow Control Conference. 2004. DOI: 10.2514/6.2004-2120
2. **Edward J.B.W.** Free Flight Measurements of the Drag and Longitudinal Stability of a Transonic M-Wing Aircraft. Bedford Library, 1964.
3. **D.A.J. van Ginneken, Mark Voskuil, Michel J.L. van Tooren.** Automated Control Surface Design and Sizing for the Prandtl Plane. AIAA 2010. DOI: 10.2514/6.2010-3060
4. **Попов С.А., Гуереш Дж., Кузнецов А.В.** Экспериментальное исследование аэродинамических характеристик крыла с треугольным выступом различных конфигураций // Изв. вузов. Авиационная техника. 2016. № 3. DOI: 10.3103/S1068799816030132
5. **Сакорнсин Р.** Оптимизация аэродинамического облика крыла гидросамолета с поплавком на конце // Труды МАИ. 2012. Вып. 57.
6. **Сакорнсин Р.** Улучшение аэродинамических характеристик комбинированного крыла путем добавления треугольного выступа // Труды МАИ. 2013. Вып. 65.
7. **Сакорнсин Р.** Аэродинамические характеристики крыла с выступом при разных углах отклонения выступов и различных компоновках крыла гидросамолета в местах соединения // Труды МАИ. 2013. Вып. 70.
8. **Johnson C.S., Barakos G.N.** Optimizing Rotor Blades with Approximate British Experimental Rotor Program Tips // Journal of Aircraft. 2014. Vol. 51. № 2. DOI: 10.2514/1.C032042
9. **Kandil O.A., Mook D.T., Nayfeh A.H.** Subsonic Loads on Wings having Sharp Leading Edges and Tips // Journal of Aircraft. 1976. Vol. 13. № 1. DOI: 10.2514/3.44512
10. **Fung Y.C.** On the Behavior of a Sharp Leading Edge // Journal of the Aeronautical Sciences. 1953. Vol. 20. Pp. 644–645. DOI: 10.2514/8.2773
11. **Whitcomb Richard T.** A Design Approach and Selected Wind Tunnel Results at High Subsonic Speeds for Wing-tip Mounted Winglets. NASA Technical Note D-8260. 1976.
12. **Nicolas R. El Haddad and Luis Gonzalez.** Aerodynamic Design of a Winglet for the Dassault Falcon 10. AIAA 2016. DOI: 10.2514/6.2016-0776
13. **Takenaka K., Hatanaka K., Yamazaki W., Nakahashi K.** Multidisciplinary Design Exploration for a Winglet // AIAA Journal of Aircraft. 2008. DOI: 10.2514/1.33031

СВЕДЕНИЯ ОБ АВТОРАХ

Гуереш Джахид, аспирант и ассистент кафедры аэродинамики и процессов теплообмена летательных аппаратов МАИ, guaero.tech@gmail.com; d.gueraiche@mai.ru.

Попов Сергей Александрович, кандидат физико-математических наук, доцент кафедры аэродинамики и процессов теплообмена летательных аппаратов МАИ, flowmech@gmail.com.

Поступила в редакцию
Принята в печать

10.11.2017
28.12.2017

Received
Accepted for publication

10.11.2017
28.12.2017